Article

ASSESSMENT OF URBAN HEAT ISLAND IN THE NORTH-EASTERN STATE CAPITALS IN BRAZIL USING SENTINEL SATELLITE DATA – 3 SLSTR

Rodrigo Fernandes [1,] *, Antonio Ferreira [2], Victor Nascimento [3,] and Marcos Freitas [1]

[1] Postgraduate Program in Remote Sensing (PPGSR), Federal University of Rio Grande do Sul (UFRGS), Porto Alegre 91501-970, RS, Brazil; passos.fernandes@ufrgs.br (R.F.); mfreitas@ufrgs.br (M.F.)
[2] Federal University of Ceará (UFC), Institute of Marine Sciences (LABOMAR), Fortaleza 60165-081, CE, Brazil; antonio.ferreira@ufc.br (A.F.)
[3] Center for Engineering, Modeling, and Applied Social Sciences, Federal University of ABC (UFABC), Santo André 09210-580, SP, Brazil; victor.fernandez@ufabc.edu.br (V.N.)
* Correspondence: passos.fernandes@ufrgs.br

Abstract: The Surface Urban Heat Island (UHI) is caused by the difference in temperature between the urban and its surrounding areas. However, in the scientific literature, there is no solid methodology defining urban and non-urban areas, which is essential to estimate the SUHI with greater accuracy. This study uses the official national urban areas limit, to obtain the SUHI more accurately on the nine northeastern Brazilian capitals. The land surface temperature was obtained using the Sentinel 3 satellite data for the years 2019 and 2020. Afterward, the maximum and average SUHI, and the complementary indexes were calculated, such as the Urban Thermal Field Variation Index (UTFVI) and the Thermal Discomfort Index (TDI) for the urban areas and their surrounding areas. The Maximum and Average SUHI, obtained values between 1.85 and 8.25 and -4.92 and 2.59 degree difference, respectively, proving the SUHI existence in the study areas. The UTFVI, with values between 0.010 and 0.040, expresses how bad the eco-environmental spaces of urban are. The TDI, with values between 24.61 and 28.89 ºC, expresses the population's thermal comfort. Therefore, this study provides a better understanding of the surface UHI pioneeringly for the Brazilian Northeast Region.

Keywords: Surface Urban heat island. Northeastern region. Sentinel 3. Eco-environmental spaces. Thermal comfort.

1. Introduction

Solar radiation keeps planet Earth warm, essential for maintaining life as we know it. It assists in evaporation, transpiration, and photosynthesis, which are natural and indispensable for this warming. As a result, radiation is considered the main meteorological element. Its study for remote sensing extends to energy balance effects, the greenhouse effect, global climate change, and urban heat islands (UHI). This last one is one of the most studied urban climate effects [1-3].

While the greenhouse effect of warming occurs naturally, it has increased lately [4]. Otherwise, urban heat islands arise mainly due to anthropic issues [5]. Therefore, changes in the urban structure over the years, influenced by the population migration from the rural to the urban areas, have contributed to undermining the carrying capacity of the natural space, generating considerable negative environmental impacts. The most common problems are associated with using common building materials that absorb more radiation than in less urbanized rural areas, causing the phenomenon known as Urban Heat Island [6].

 doi:10.20944/preprints202304.0045.v1

Several factors can contribute to UHI formation, such as the city's materials impermeability, dark components, geometrically unfavorable buildings for proper air circulation, man-made heat and pollution sources, and low wind speeds [7-9].

In addition, the UHI is defined as the difference between the air temperature within the urban area and its surroundings [10]. These high-temperature effects are direct consequences of changes in the surface energy balance. They are reinforced by the climate change impact, which affects people's psychological and physiological well-being and controls daily mood and financial behaviors [11]. Moreover, inhabitants of major tropical and semiarid cities often experience the UHI phenomenon more often and more intensely since the cities in the tropics are already naturally warmer [12].

According to [13], the use of orbital images has become widespread with the satellite's development advancement, increasing the spatial, spectral, and temporal resolution. In addition, these images have been essential in evaluating environmental impacts and are a powerful tool for monitoring changes in urban space. For example, one way to monitor the urban climate is through thermal infrared bands. Once part of the solar radiation is absorbed and emitted by the urban surface, it is up to the satellite sensors operating in the thermal infrared range to capture this spectral response and then, with appropriate corrections, estimate the Land Surface Temperature (LST), which can be used to detect the surface UHI (SUHI) [14,15].

Several authors have studied SUHI detection with different approaches at spatial, temporal, and spectral scales or tested which satellite sensor is most appropriate [16-20]. However, most of these studies focus only on a single locality where the definition of the urban and rural areas is tailored for each case study, making difficult comparisons between localities in different parts of the world. However, there is not only one methodology to define a non-urban area, and its several Land Use and Land Cover (LULC) classes identification is essential for the SUHI estimation once the wrong classification can lead to UHI values underestimation or overestimation. Therefore, the classification of non-urban and urban areas is a challenge nowadays.

This study aims to analyze SUHI values for all capital cities of northeastern Brazil using the Urban Thermal Field Variation (UTFVI), and the Thermal Discomfort Indices (TDI) obtained using the Sentinel 3 satellite, SLSTR sensor, for the years 2019 and 2020. The main novelty of this study is this methodology application for the northeast Brazilian region, which is a semiarid region. In addition, the importance of this study is related to the Sustainable Development Goals (SDG) 11, which aims to achieve more inclusive, safe, and resilient human settlements [21].

2. Study Area

The study area is the northeastern (NE) Brazilian capitals, Fortaleza, Maceió, Salvador, São Luís, João Pessoa, Recife, Teresina, Natal, and Aracaju, located in the Bahia (BA), Maranhão (MA), Paraiba (PB), Pernambuco (PE), Piauí (PI), Rio Grande do Norte (RN), Sergipe (SE) states, respectively (Figure 1).

Preprints (www.preprints.org) | NOT PEER-REVIEWED | Posted: 4 April 2023 doi:10.20944/preprints202304.0045.v1

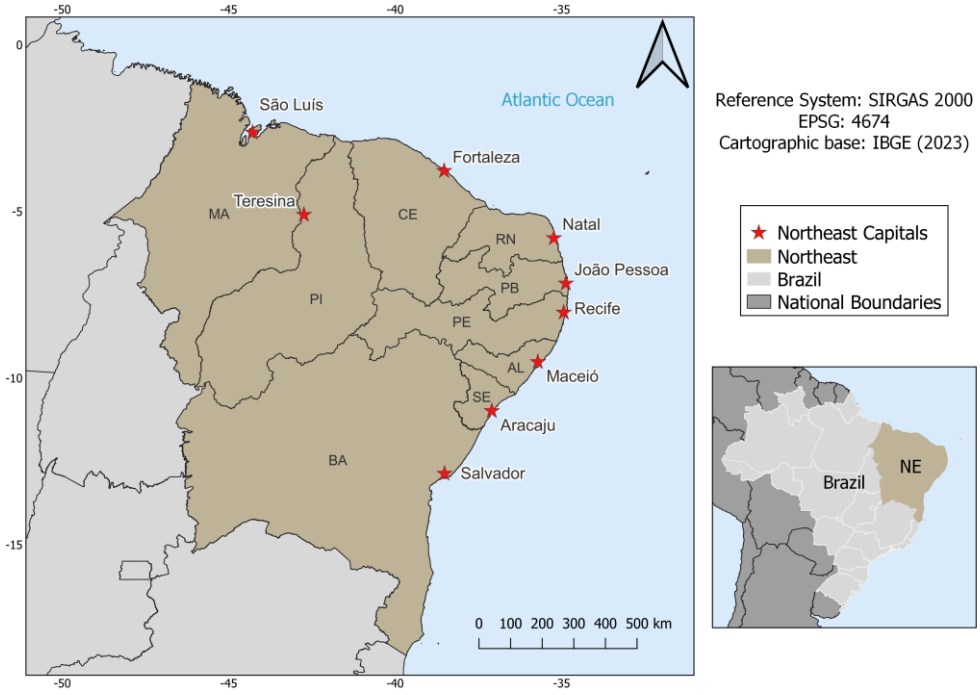

Figure 1. Study area highlighting the nine capital cities of the Brazilian Northeast Region.

These capitals were chosen because they have diverse areas size, populations, and demographic densities [22] (Table 1). For example, Salvador has the largest population, but Fortaleza has the highest demographic density. Also, Teresina is the only one not on the coast. In addition, the Brazilian Northeast has few studies on the subject. Furthermore, an analysis such as this study for cities affected by the semiarid climate would be fundamental to mitigate the SUHI phenomena.

Table 1. Brazilian Northeast capitals characteristics.

Capitals	Areas (km²)	Estimated population	Demographic density (hab/km²)
Fortaleza-CE	312.353	2,686.612	8601.204
Maceió-AL	509.320	1,025.360	2013.194
Salvador-BA	693.453	2,886.698	4162.788
São Luís-MA	583.063	1,108.975	1901.981
João Pessoa-PB	210.044	817,511	3892.094
Recife-PE	218.843	1,653.461	7555.467
Teresina-PI	1,391.293	868,075	623.934
Natal-RN	167.401	890,480	5319.443
Aracaju-SE	182.163	664,908	3650.072

3. Materials and Methods

A flowchart of the methodology steps taken in this study is shown in (Figure 2).

Preprints (www.preprints.org) | NOT PEER-REVIEWED | Posted: 4 April 2023 doi:10.20944/preprints202304.0045.v1

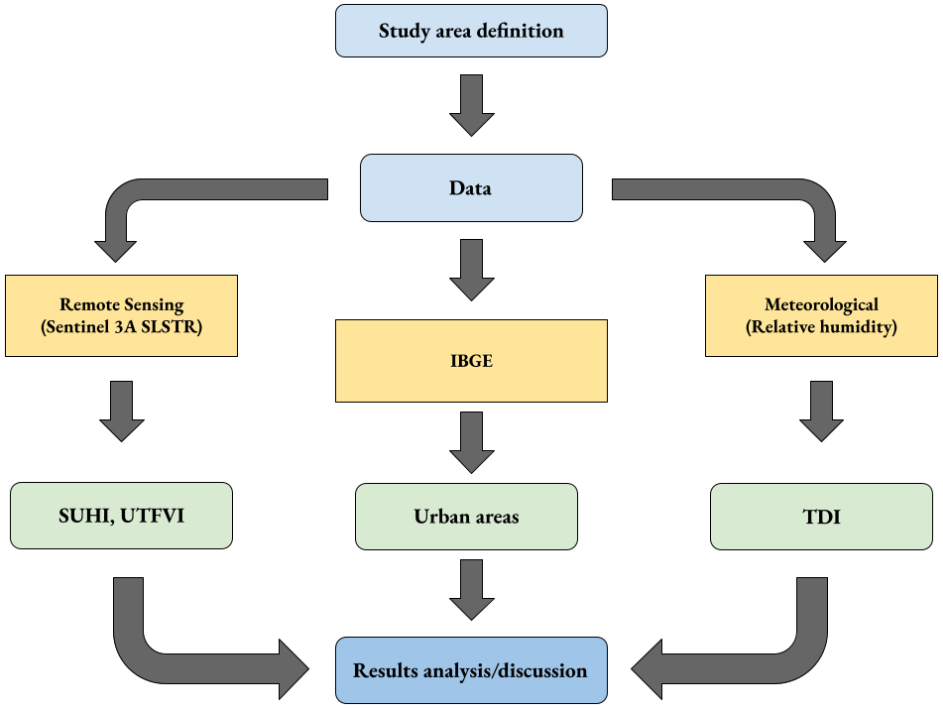

Figure 2. Flowchart of the methodology

3.1. Remote Sensing Data

This study used remote sensing data from the Sentinel – 3A satellite of the European Space Agency (ESA) obtained from November 2019 to November 2020 for each northeastern Brazilian capital (Table 2). The SUHI was analyzed with the land surface temperature (LST) product generated from the SLSTR sensor, with 1 km of spatial resolution in the thermal band, presenting a Polar/Heliosynchronous orbit, altitude of 815 km, an inclination of 98.6° and with a revisit period of 27 days. The LST data obtained only required cutouts for the study regions, and an appropriate georeferencing for each, in which it already comes with atmospheric and geometric corrections. Night thermal infrared images were used, because the SUHI effects are usually strong in this period, due to the heat up and energy stored by impervious surfaces and buildings during the day, which is slowly restored in the heat form at night [23].

Table 2. Day and time of Sentinel – 3 image acquisition for the Northeastern state capitals.

Capital	Data	Hour (GMT)
Fortaleza-CE	14/11/2020	00:21
Maceió-AL	25/02/2020	23:00
Salvador-BA	28/02/2020	23:22
São Luís-MA	29/12/2020	00:55
João Pessoa-PB	28/01/2020	23:26
Recife-PE	28/01/2020	23:26
Teresina-PI	27/11/2019	23:33
Natal-RN	25/02/2020	23:00
Aracaju-SE	28/02/2020	23:22

3.2 . Meteorological Data

This study used Relative humidity data extracted from meteorological stations in each capital of the study area (Figure 3). These data were obtained from the National In-

Preprints (www.preprints.org) | NOT PEER-REVIEWED | Posted: 4 April 2023 doi:10.20944/preprints202304.0045.v1

stitute of Meteorology (INMET) at (https://bdmep.inmet.gov.br/) for all the Brazilian northeast capitals to calculate the Thermal Discomfort Indices (TDI).

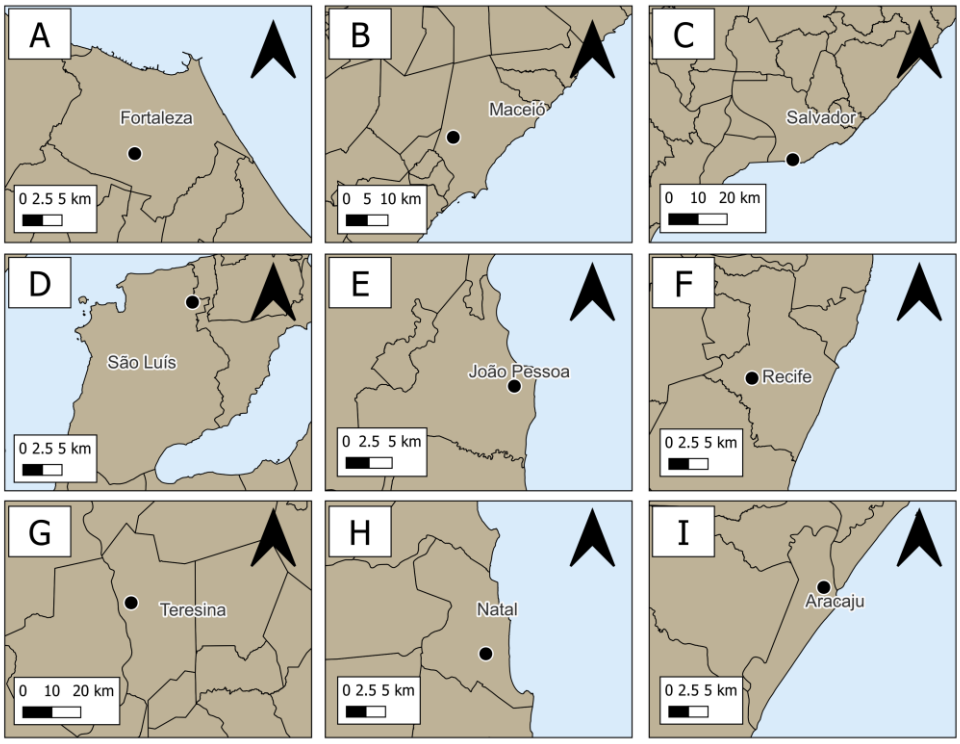

Figure 3. Location of the weather stations used for the northeastern Brazilian capitals. A) Fortaleza(Lat. -3.815701; Lon. -38.537792), B) Maceió(Lat. -9.55111111; Lon. -35.77027777), C) Salvador(Lat. -13.005515; Lon. -38.50576), D) São Luís(Lat. -2.52666666; Lon. -44.21361111), E) João Pessoa(Lat. -7.165409; Lon. -34.815627), F) Recife(Lat. -8.05928; Lon. -34.959239), G) Teresina(Lat. -5.03472221; Lon. -42.80138888), H) Natal(Lat. -5.83722221; Lon. -35.20805555), and I) Aracaju(Lat. -10.952413; Lon. -37.05433).

3.3. Methodology

3.3.1. Surface Urban Heat Island and its Surroundings Estimation

The nighttime Land Surface Temperature (LST) data was retrieved from Sentinel-3 satellite images and were used according to [24]:

$$\text{Maximum SUHI} = (\text{Maximum Urban LST} - \text{Average Surrounding LST}) \quad (1)$$

$$\text{Average SUHI} = (\text{Average Urban LST} - \text{Average Surrounding LST}) \quad (2)$$

where: the Maximum Urban LST is the hottest pixel in the urban area. The Average Urban LST and the Average Surrounding LST are the average temperatures of all the pixels in the urban and its surroundings, respectively.

The Sentinel Application Platform (SNAP) software, provided by ESA for processing and analyzing images from the Sentinel series satellites, was used to analyze the statistical parameters of the images used in this study.

3.3.2. Urban and Surroundings areas selection

To identify the urban area, [24] propose using a land cover map with an explicit representation of the urban agglomeration provided by the European Space Agency [25]. However, the official limits of the capital urban areas from the Brazilian Institute of Ge-

Preprints (www.preprints.org) | NOT PEER-REVIEWED | Posted: 4 April 2023 doi:10.20944/preprints202304.0045.v1

ography and Statistics (IBGE), available at (https://www.ibge.gov.br/geociencias/downloads geociencias.html were used in this study.

Afterward, the surrounding areas were split into three different reference classes: the urban adjacent (Ua), the future urban adjacent (FUa), and the peri-urban (PUa). Furthermore, the widths of these surroundings WUa, WFUa, and WPUa, respectively, were calculated as follows according to [24]:

$$WUa = 0.25\ A½ \quad (3)$$

$$WFUa = 0.25\ AWUa½ \quad (4)$$

$$WPUa = 1.5\ A\ 1/2 - WFUa - WUa \quad (5)$$

in addition, "A" represents the urban area and AWUa is the sum of the areas of A and Ua.

The representation of the areas adjacent to the urban area was generated by the Michael Minn Quantum GIS (MMQGIS) "create buffers" tool of the QGIS software version 3.16.1. Figure 4 represents the adjacent areas in the form of buffers for the cities.

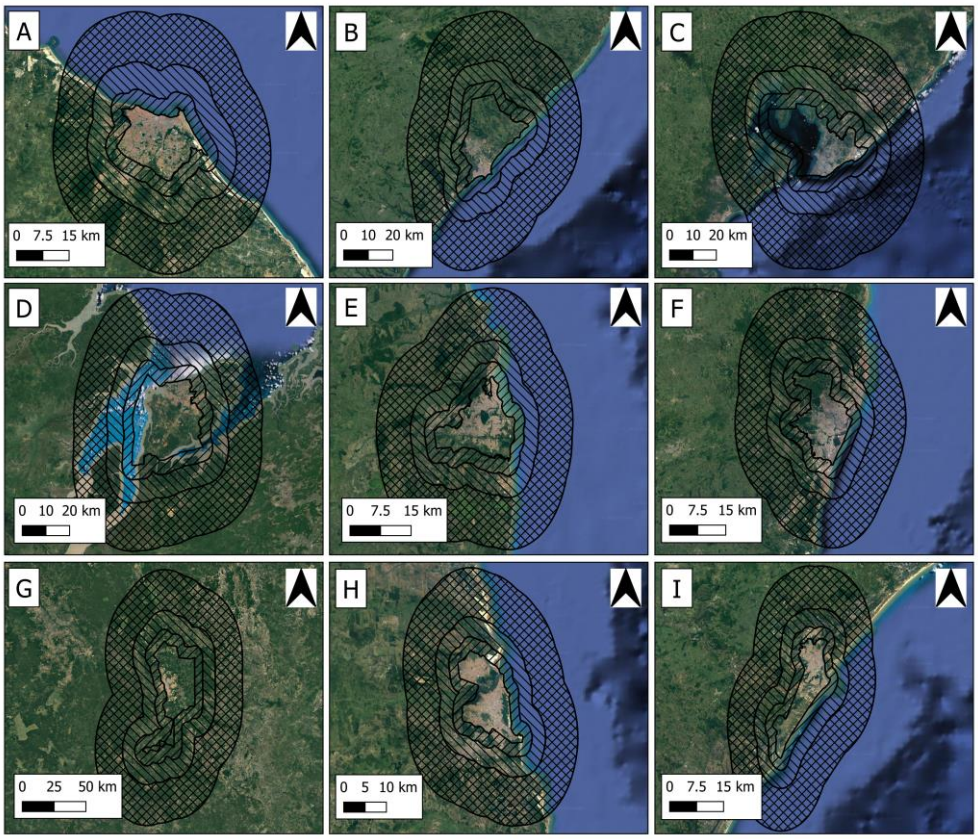

Figure 4. Urban and surroundings areas WUa, WFUa, WPUa, respectively for all the northeastern Brazilian capitals. A) Fortaleza, B) Maceió, C) Salvador, D) São Luís, E) João Pessoa, F) Recife, G) Teresina, H) Natal, and I) Aracaju.

3.3.3. UTFVI and TDI indexes

In addition, to complement the SUHI analysis, additional indices were considered.

The first was the UTFVI, which is the most widely used for ecological thermal assessment of city environments due to its relationship with LST, as well as considering the

Preprints (www.preprints.org) | NOT PEER-REVIEWED | Posted: 4 April 2023 doi:10.20944/preprints202304.0045.v1

thermal impacts of different subareas, as applied by [26], describing the effects of the index in their analysis area quantitatively.

The equation below describes the UTFVI calculation, according to [27, 28]:

$$UTFVI = 1 - (Tmean / Ts) \quad (6)$$

where, Ts is the LST in Kelvin, obtained from Sentinel - 3 satellite data, of a given pixel in the urban area (A), and Tmean is the LST mean of the whole study area in Kelvin.

The maximum and average urban heat island describes the temperature effect on the entire study area. At the same time, the UTFVI is used to assess the effect of each pixel located only inside the urban area. In addition, the index is divided into six levels (Table 3) by SUHI occurrence phenomenon related to the urban environment ecological evaluation [29, 30].

Table 3. Thresholds values of UTFVI and ecological evaluation index.

UTFVI	SUHI phenomenon	Ecological evaluation index
<0	None	Excellent
0 – 0.005	Weak	Good
0.005 – 0.010	Meddle	Normal
0.010 – 0.015	Strong	Bad
0.015 – 0.020	Stronger	Worse
>0.020	Strongest	Worst

Additionally, we know that UHI affects people's health, so the TDI measures the human body's reaction to a combination of heat and humidity. According to [31], this index allows the estimation of people's thermal comfort concerning the environment they live. The TDI is described as (Equation 7) accordingly proposed by [32]:

$$TDI = LST - (0.55 - 0.055\ RH)\ (LST - 14.5) \quad (7)$$

where LST is the land surface temperature at a given pixel of A, this should be presented in degrees Celsius, and finally, RH is the relative humidity in %. According to [33], the TDI is divided into ten categories, as shown in Table 4.

Table 4. TDI classification values.

TDI categories	Temperature (ºC)
Hyper Glacial	<-40
Glacial	-39.9– -20
Extremely cold	-19.9– -10
Very Cold	-9.9– -1.8
Cold	-1.7– 12.9
Cold	13 – 14.9
Comfortable	15 – 19.9
Hot	20 – 26.4
Very Hot	26.4– 29.9
Torrid	>30

4. Results and Discussion

The SUHI maximum and average values, in addition to UTFVI and the TDI, should be interpreted as results of the day and time obtained from each data analyzed. Some points of vulnerability were noticed in the capitals studied, such as high-temperature values for urban areas, worrisome results of the ecological indexes for cities for cities, and

Preprints (www.preprints.org) | NOT PEER-REVIEWED | Posted: 4 April 2023 doi:10.20944/preprints202304.0045.v1

thermal sensations harmful to humans. Identifying these vulnerabilities becomes even more important to reach SGD 11 and, in a warming context world, the trend of global temperature increase is linear at 0.18 K per decade [34], and, according to the most recent report of the Intergovernmental Panel on Climate Change (IPCC), the world has already warmed by 1.1 °C, and is likely to exceed 1.5 °C by the 2030s [4].

4.1. Surface Urban Heat Island

4.1.1. Maximum and average urban heat island

The maximum and average SUHI values for all the northeastern Brazilian capitals are represented in (Figures 5 and 6), respectively, considering the urban adjacent (Ua), the future urban adjacent (FUa), and the peri-urban (PUa).

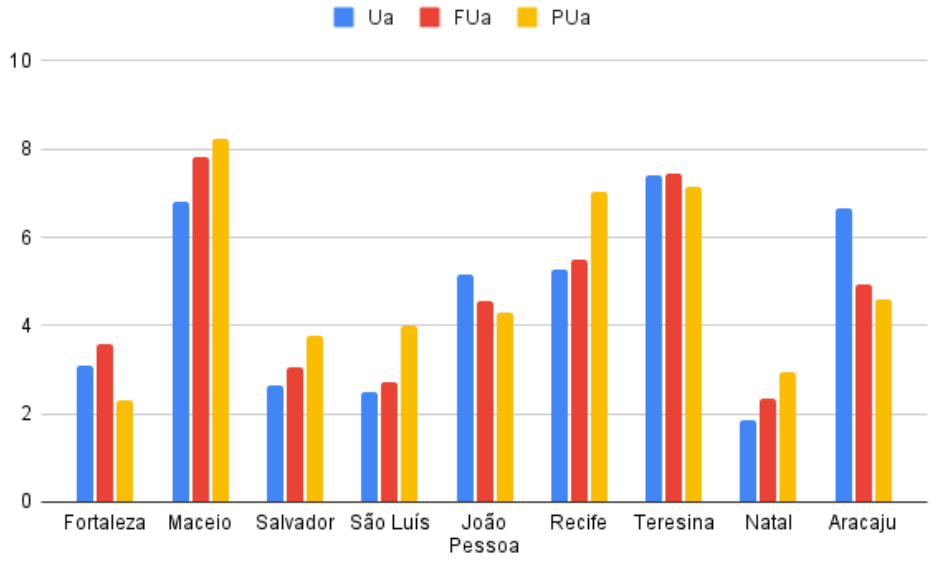

Figure 5. Maximum SUHI for Ua, FUa, and PUa.

An increasing trend in SUHI values in accordance with proximity to the capital was found in the cities of Maceió, Salvador, São Luis, Recife, and Natal. In contrast, a decreasing trend in relation to the capital was found in Fortaleza, João Pessoa, Teresina, and Aracaju.

In addition, to the maximum SUHI values, the same analysis was made with the average SUHI values and is shown in (Figure 6).

Preprints (www.preprints.org) | NOT PEER-REVIEWED | Posted: 4 April 2023 doi:10.20944/preprints202304.0045.v1

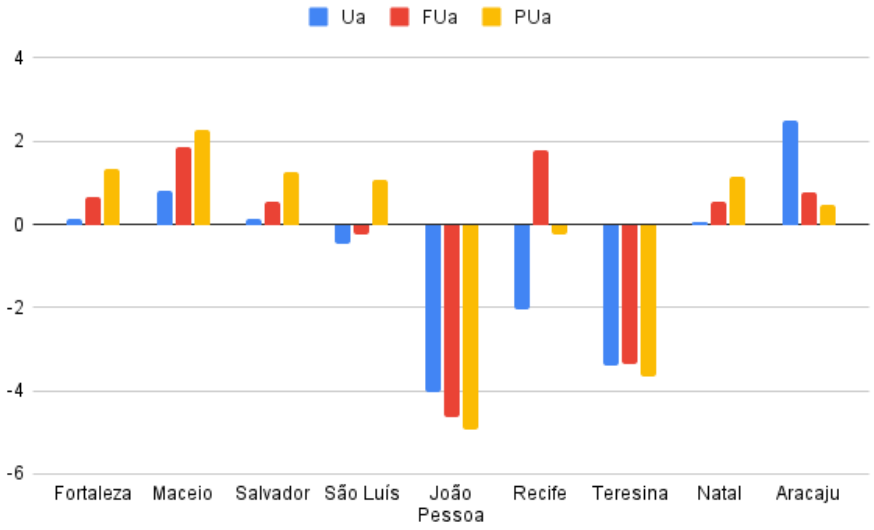

Figure 6. Average SUHI for Ua, FUa, and PUa.

For example, Fortaleza began to present its areas closest to the urban center with higher temperatures, around 27 °C. Even so, Maceió, Salvador, São Luís, and Natal are configured with the expected values, in which the urban area has higher temperatures. In contrast, Recife continued with its lower value in Ua, but the FUa obtained a higher value concerning Ua and PUa, thus being colder in this zone. In contrast, for Teresina, the FUa value was lower, thus characterizing it as a warmer zone, and João Pessoa and Aracaju obtained their warmest zones in their areas farther from the respective urban regions.

Therefore, considering that areas with vegetation and bodies of water mitigate the accumulated heat, while areas with exposed soil and certain construction materials increase the temperature [35-41], the hypotheses were raised to explain the results obtained in the Northeastern capitals, with the support of LULC images from MapBiomas [42], Figure 7.

Preprints (www.preprints.org) | NOT PEER-REVIEWED | Posted: 4 April 2023 doi:10.20944/preprints202304.0045.v1

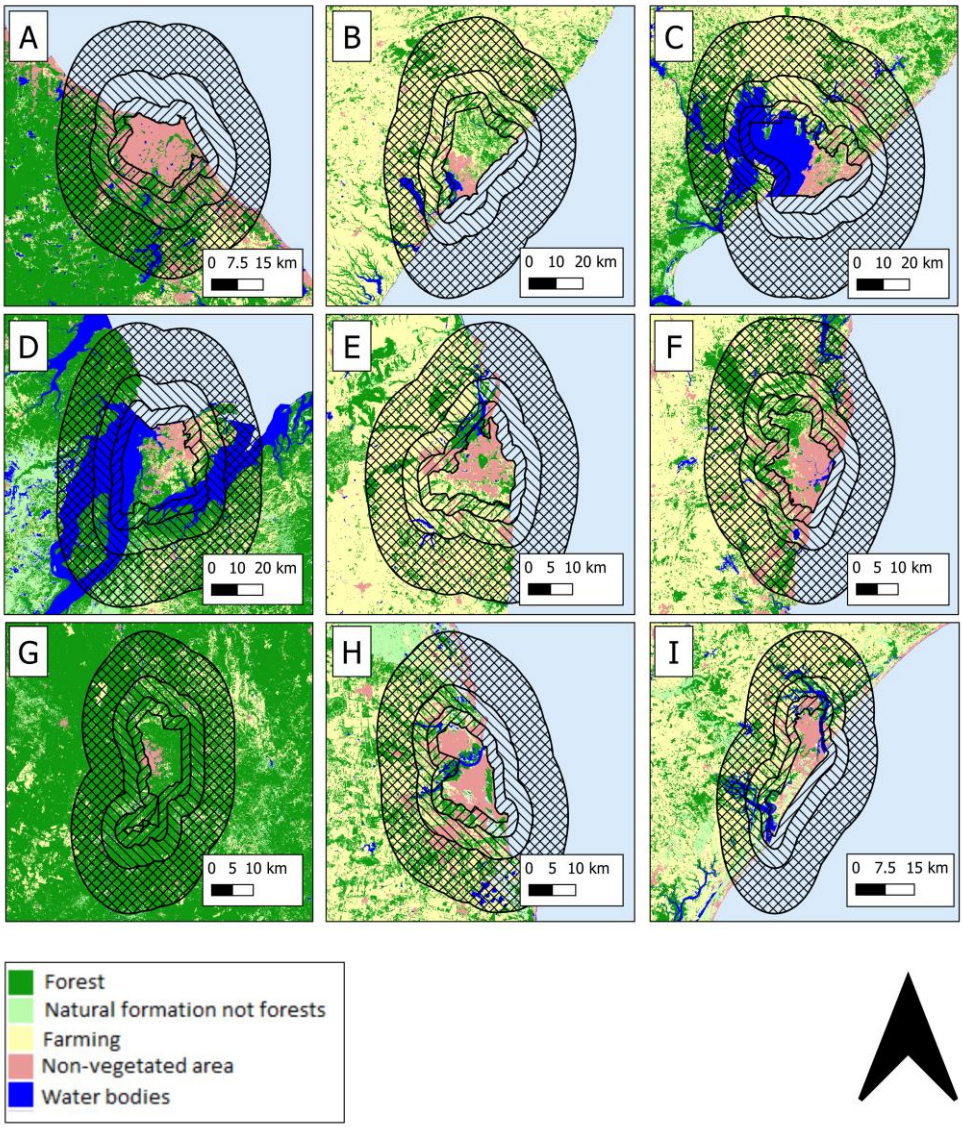

Figure 7. LULC , respectively for all the northeastern Brazilian capitals. A) Fortaleza, B) Maceió, C) Salvador, D) São Luís, E) João Pessoa, F) Recife, G) Teresina, H) Natal, and I) Aracaju.

Figure 8 shows the capital cities with the respective LST.

Preprints (www.preprints.org) | NOT PEER-REVIEWED | Posted: 4 April 2023 doi:10.20944/preprints202304.0045.v1

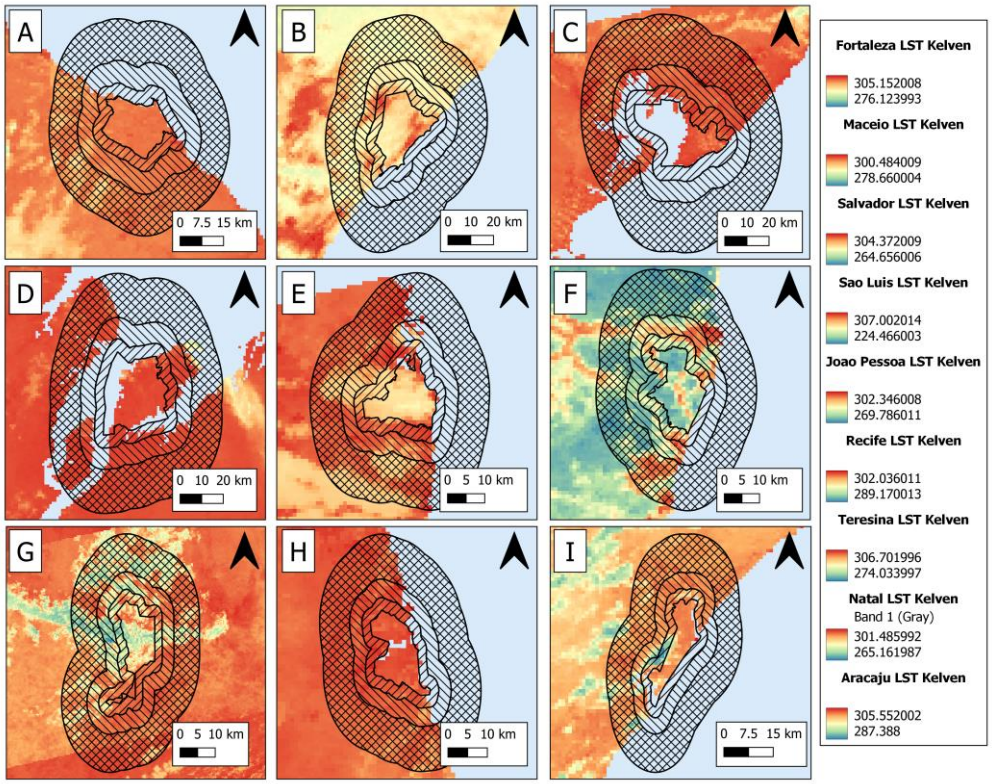

Figure 8. LST (Kelvin) of the northeastern Brazilian capitals and their respective surroundings areas.

Analyzing the Fortaleza maximum SUHI, a high temperature may have occurred in the furthest region of the urban area, at PUa, with a value of 2.31, because the hottest pixel of this area had a very high temperature of approximately 30.96 °C. The region is where Aquiraz is located, a well-traveled and paved metropolitan region (Figure 4A e 7A), which may explain the high value found. But in compensation, in the average SUHI, the pixel temperatures in the city's urban area has the highest values, corresponding to 0.13 degree difference, explaining the high temperature near urban areas.

The areas adjacent to Maceió are heavily vegetated and have many bodies of water in the westernmost portion, which may explain the high temperature in urban areas compared to the furthest areas in both the maximum and average SUHI calculation values of 6.79 and 0.82 degree difference, respectively.

Similar to Maceió, Salvador has a water body to the west of the city and many vegetated areas in its suburban areas, besides having a few neighboring towns in the suburban areas. While in the average SUHI, the urban area of Salvador is explicit with temperatures higher than its surroundings, with a value of 2.66 in the maximum SUHI in Ua. However, FUa has very similar values, which can be explained by the presence of a city near Uf, which is responsible for this temperature increase.

In the analysis of the maximum SUHI, Ua is lower among the three reference areas, with a value of 2.48. Therefore, the urban areas present higher temperatures than their surroundings, where the same occurred for the average SUHI, with a value of 0.46. It is worth noting that the areas around the city are vegetated and have water bodies.

With the analysis of the maximum and average SUHI of João Pessoa, it is possible to verify that the PUa temperatures were higher for the other regions and with respect to the urban area, corresponding to 4.28 and -4.92, respectively.

These results may have occurred because PUa is an area with much-exposed soil, besides presenting sites with housing developments, justifying the high temperatures. Regarding the milder temperatures in the city, the region is well-wooded in some loca-

 doi:10.20944/preprints202304.0045.v1

tions, more specifically when we look at the central part of the city (Figure 4E e 7E), where the Botanical Garden is located, as shown in Figure 3, this being a 5 km² area with remnant Atlantic Forest vegetation [43].

In the Recife case, in calculating the maximum and average SUHI, the values obtained among the reference regions were lower for Ua, with 5.21 and -2.03, respectively. However, for the other areas, PUa is still lower than Uf, thus having higher temperature values in PUa concerning it. Ua and PUa can explain this by covering more areas with exposed soil and built-up regions in neighboring cities.

The values of the defined areas in Teresina were very close, all around 7. This magnitude may have occurred because the urban and its surrounding areas present similar characteristics to the area near the urban core, such as the presence of exposed soil in the surroundings, as shown in Figure 4G. However, the hottest areas were near the PUa. In fact, vegetation occurs near the city and in the closest adjacent areas, still with the presence of a water body, although this is losing its space to the urban constructions.

According to [24], a similar case of very close values of Ua, FUa, and PUa occurred. As presented in their work, the cities of Athens, Shanghai, Calcutta, and Dammam presented the same conditions as Teresina, having similar surroundings to the urban area.

In Natal, the values of Ua were lower for the two calculations of maximum and average SUHI, 1.85 and 0.06, respectively, in which the city's urban area is hot concerning its surroundings, considering that it has plenty of vegetation in the adjacent regions. However, despite a significant water body in the city, it is surrounded by buildings and constructions, in addition to the few green areas in the city.

Also, in 71 cities analyzed in the [24] study, 68 showed similar results to Natal, where their maximum and average SUHI, in both cases, were at high temperature values near the urban concerning adjacent areas.

In the case of Aracaju, the PUa presented the lowest values for the two calculations of maximum and average SUHI, with 4.61 and 0.46, respectively, especially when analyzing the average. In addition, the city has some vegetated areas and riverbanks with riparian forests. Its immediate surroundings also have these elements, which can justify the occurrence of lower temperatures concerning PUa.

4.3. Thermal Indexes

4.3.1. Urban Thermal Field Variation Index

The UTFVI values were the highest for João Pessoa, Recife, and Teresina (Figure 9). These values were above 0.020, possessing a very strong Heat Island phenomenon and their ecological indexes being considered the worst, according to (Table 3). Moreover, Maceió and Aracaju presented a strong phenomenon, and the remaining capitals presented medium to strong phenomena. However, it is worth noting that these results are for the regions of the city with the hottest pixels in each urban area, thus configuring that it has an average, strong and/or very strong Urban Heat Island Phenomenon in that specific region of the analyzed city area, and therefore also has a normal, poor and/or bad eco-environment.

Preprints (www.preprints.org) | NOT PEER-REVIEWED | Posted: 4 April 2023 doi:10.20944/preprints202304.0045.v1

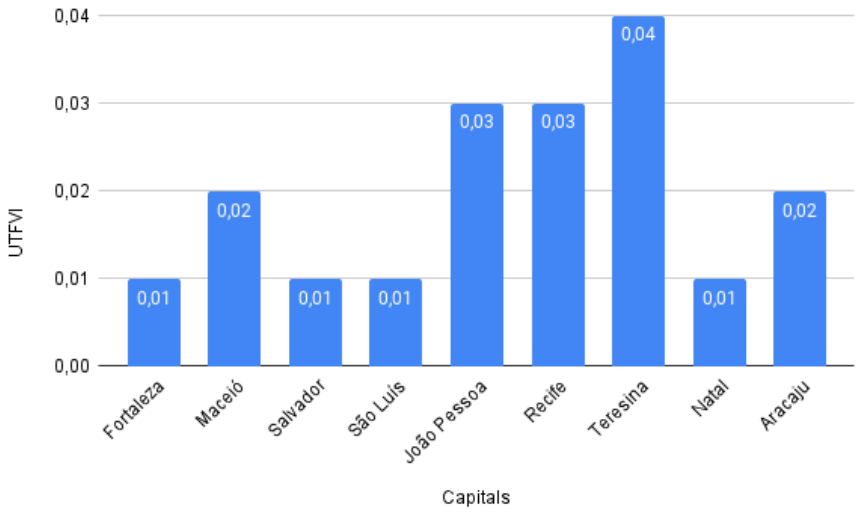

Figure 9. UTFVI values for the Northeast Brazilian capitals.

4.3.2. Thermal Discomfort Index

The maximum and average Thermal Discomfort Index (TDI) is presented in (Figure 10), indicating the influence of people's perception of the temperature around them.

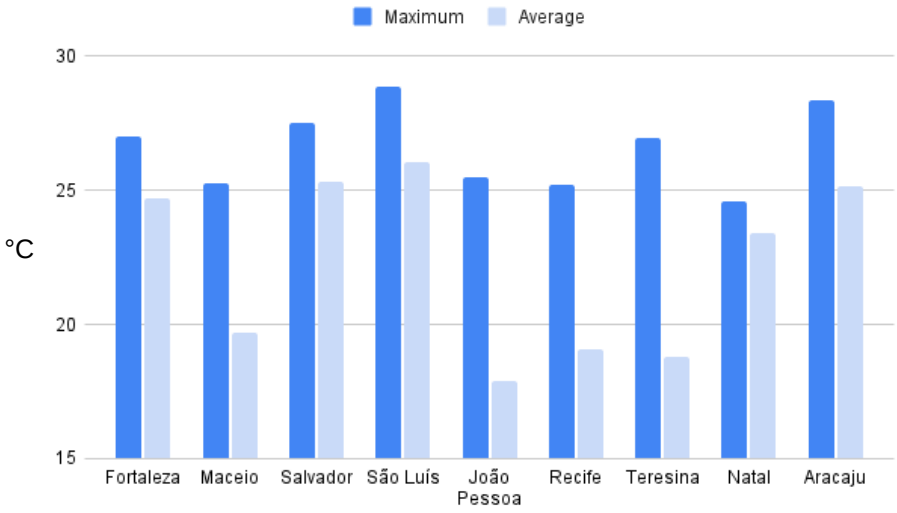

Figure 10. Maximum and Average TDI values for the Northeast Brazilian capitals.

Regarding TDI, the hottest pixels in the urban area the thermal discomfort was Very Hot for Fortaleza, Salvador, São Luís, João Pessoa, Teresina and Aracaju. The remaining capitals obtained a hot classification.

These values show that all the capitals, for their hottest areas, have thermal comfort above 20 ºC, above what is comfortable for the population, as shown in (Table 4). Furthermore, as [44] indicated, the pattern values above 21 °C, less than 50% of the population feels discomfort, which, according to [45], discomfort is understood as sensations of heat and cold, uncomfortable feelings of unease.

The average TDI, on the other hand, to the urban area average pixels, the classification Very Hot was only for São Luís; Hot for Salvador, Aracaju, Fortaleza, Natal, and Comfortable for Maceió, Recife, Teresina, and João Pessoa.

Preprints (www.preprints.org) | NOT PEER-REVIEWED | Posted: 4 April 2023 doi:10.20944/preprints202304.0045.v1

These results demonstrated that the average pixels in the urban areas in most capitals, five of them, present thermal comfort above 20 ºC, being above what is comfortable for the population and was the maximum thermal discomfort.

4.5. Summary of Results

A summary of the main results obtained for the capital cities assessed in this study is presented in (Table 5). The average LST is presented in Celsius of the urban area. Columns 3 to 8 represent the values of Ua, FUa, and PUa for the maximum and average UTFVI, respectively. The indexes are represented by their maximum values, and finally, the date is the day of the image obtained by the Sentinel 3 satellite.

Table 5. Summary table with the main results for all northeastern Brazilian capitals.

City	Average LST	Max SUHI Ua	Max SUHI FUa	Max SUHI PUa	Ave SUHI Ua	Ave SUHI FUa	Ave SUHI PUa	Max UTFVI	Max TDI	Date
Fortaleza	28.39	3.10	3.57	2.31	0.13	0.67	1.35	0.01	26.99	14/11/20
Maceió	21.13	6.79	7.83	8.25	0.82	1.86	2.28	0.02	25.24	25/02/20
Salvador	28.18	2.66	3.07	3.77	0.14	0.55	1.25	0.01	27.50	28/02/20
São Luís	27.71	2.48	2.71	4.00	-0.46	-0.23	1.06	0.01	28.89	29/12/20
João Pessoa	19.62	5.15	4.55	4.28	-4.05	-4.65	-4.92	0.03	25.52	28/01/20
Recife	20.89	5.28	5.51	7.05	-2.03	1.80	-0.26	0.03	25.23	28/01/20
Teresina	21.26	7.39	7.43	7.14	-3.40	-3.36	-3.65	0.04	26.94	27/11/19
Natal	25.82	1.85	2.33	2.94	0.06	0.54	1.15	0.01	24.61	25/02/20
Aracaju	29.25	6.65	4.92	4.61	2.50	0.77	0.46	0.02	28.37	28/02/20

As already observed in the Results, the maximum and average SUHI values for Natal-RN for the three reference areas were similar to the 68 cities studied by [24]. As seen in Table 5, the maximum and average SUHI values for Maceió-AL, Salvador-BA, and São Luís - MA were similar to those presented by Natal-RN.

Notably, in the city of Teresina, as seen in Table 5, the maximum and average SUHI values were all very close.

5. Conclusions/Concluding Remarks

Obtaining land surface temperature from remote sensing allowed us to estimate the UHI and its influence in three adjacent city areas. Still, a fine selection of these urban surroundings is necessary to detect better and assess these temperature differences. Taking these facts into consideration, we used the methodology to more accurately calculate the SUHI effects in the cities of Fortaleza-CE, Maceió-AL, Salvador-BA, São Luís-MA, João Pessoa-PB, Recife-PE, Teresina-PI, Natal-RN, and Aracaju-SE in the northeastern region of Brazil.

In this study, local data from IBGE was used to obtain the urban area and thus locate the reference areas of the surroundings, the urban adjacent (Ua), the future urban adjacent (FUa), and the peri-urban (PUa), discovered by calculations that depend exclusively on the original urban area. Besides being performed the calculation of the maximum and average SUHI of the urban area for each reference area.

With the remote sensing data obtained, most capitals got higher SUHI values than their surroundings. In making this inference, factors such as lack of vegetated areas, areas without the presence or with water bodies "suffocated" by the city, regions with exposed soil, and the presence of materials that retain a lot of heat and energy from the sun were taken into consideration. These considerations are reasons for the increase in urban areas and their surroundings, which are present in the study areas.

The Urban Thermal Field Variation Index (UTFVI) and the Thermal Discomfort Index (TDI) help to understand each study area. , In the UTFVCI, it is verified that for the hottest regions of the urban area, the capital cities present results that prove that the city space in question presents a very poor ecological index. In addition, the Thermal Discomfort Index verified thermally uncomfortable values for the population in general.

Therefore, this study helps SDG 11 to reach more and more its cherished goal. In addition, the methodology used in this study can help urban managers in future decision-making to better manage the urban environment, especially in northeastern Brazilian capitals with diverse areas, populations, and demographic density, besides being in a semiarid climate. Finally, this study could be replicated for other cities worldwide using global remote sensing data. However, it also needs local meteorological data, which is sometimes challenging to find in several cities.

Author Contributions: Conceptualization, R.F. and A.G.; methodology, R.F. and A.G.; software, R.F.; validation, A.G., V.N. and M.F.; formal analysis, R.F.; investigation, R.F., A.G and V.N.; resources, R.F.; data curation, R.F.; writing—original draft preparation, R.F.; writing—review and editing, A.G. and V.F.; visualization, R.F.; supervision, A.G. and V.F.; project administration, R.F.; funding acquisition, M.F. All authors have read and agreed to the published version of the manuscript.

Funding: This research was funded by *Coordenação de Aperfeiçoamento de Pessoal Nível Superior* (CAPES) R.F scholarship number (88887.645454/2021-00).

Acknowledgments: The authors thank the Federal University of Ceará (UFC), the Federal University of Rio Grande do Sul (UFRGS), and the Federal University of ABC (UFABC) for the support provided during this research.

Conflicts of Interest: The authors declare no conflict of interest.

References

1. Oliveira, A.; Lopes Oliveira, A.; Lopes, A.; Niza, S.; Soares, A. An Urban Energy Balance-Guided Machine Learning Approach for Synthetic Nocturnal Surface Urban Heat Island Prediction: A Heatwave Event in Naples. Sci. *Total Environ*. **2022**, *805*, 15013
2. Bechtel, B.; Demuzere, M.; Mills, G.; Zhan, W.; Sismanidis, P.; Small, C.; Voogt, J. SUHI Analysis Using Local Climate Zones—A Comparison of 50 Cities. *Urban Clim*. **2019**, *28*, 100451.
3. F.R.;E.D.; F.P.; *Clima Tempo*, 1nd ed.; S.A.; Embrapa Informática Agropecuária: Campinas-SP, Brazil, 2008; Volume 1, pp. 17-19.
4. IPCC. IPCC sixth assessment report. Available online: https://www.ipcc.ch/report/ar6/wg2-communities (Accessed on 15 march 2023).
5. Yang, J.; Wang, Y.; Xiu, C.; Xiao, X.; Xia, J.; Jin, C. Optimizing Local Climate Zones to Mitigate Urban Heat Island Effect in Human Settlements. J. Clean. Prod. 2020, 275, 123767.
6. Franco, F.M.; Nogueira. M.C.; Rosseti, K.A.; Nogueira, J.S. CLIMA URBANO: UM ESTUDO DE CASO PARA CLIMA TROPICAL CONTINENTAL. *Climep*, **2010**, *5*, 81-99.
7. Gartland, L. *Ilhas de calor: Como mitigar zonas de calor em áreas urbanas*. 1nd ed.; Oficina de Textos. São Paulo, Brazil, 2011. 1 pp. 8.
8. Del Serrone, G.; Peluso, P.; Moretti, L. Evaluation of Microclimate Benefits Due to Cool Pavements and Green Infraestrutures on Urban Heat Islands. *Atmosphere* **2022**, *13*, 1586.
9. Guimarães, J.T.F.; Sahoo, P.K.; e Souza-Filho, P.W.M.; da Silva M.S., Rodrigues T.M., da Silva E.F. Reis L.S., de Figueiredo M.M.J.C., Lopes K.d.S., Moraes A.M., Leite A.S., da Silva Júnior R.O., Salomão G.N., Dall'Agnol R. Landscape and Climate Changes in Southeastern Amazonia from Quaternary Records of Upland Lakes. *Atmosphere* **2023**, *14*, 621.
10. Budhiraja, B.; Gawuc, L.; Agrawal, G. Seasonality of Surface Urban Heat Island in Delhi City Region Measured by Local Climate Zones and Conventional Indicators. IEEE J. Sel. Top. Appl. Earth Obs. *Remote Sens*. **2019**, *12*, 5223–5232.
11. Quan, J. Multi-Temporal Effects of Urban Forms and Functions on Urban Heat Islands Based on Local Climate Zone Classification. Int. J. Environ. *Res. Public Health* **2019**, *16*, 35.
12. Kanga, S.;Meraj, G.; Johnson, B.A;Singh, S.J; Pv,M.N.; Farooq, M.;Kumar, P.; Marazi, A.; Sahu, N.;. Understanding the Linkage between Urban Growth and Land Surface Temperature—A Case Study of Bangalore City, India. *Remote Sens.* **2022**, *14* 14174241.
13. Trindade, P.; Michele, P.; Saldanha, D.L.; Filho, W.P.; Utilização do infravermerlho termal na análise espao temporal da temperatura de superfície e ilhas de calor urbanas. *Revista Brasileira de Cart.* **2017**, *69* 837-855.

14. Santos, T. O. d. Identificação de ilhas de calor em Recife-PE por meio de sensoriamento remote e dados meteorológicos de superfície. Master Degree, Programa de Pós-Graduação em Engenharia Agrícola – Universidade Federal de Pernambuco, Recife, 8 september 2011.
15. Shi, L.; Ling, F.; Foody, G.M.; Yang, Z.; Liu, X.; Du, Y. Seasonal SUHI Analysis Using Local Climate Zone Classification: A Case Study of Wuhan, China. *Int, J. Environ. Res.Public Health* **2021**, *18*, 7232.
16. Nassar, A.K.; Blackburn, G.A.; Whyatt, J.D. Dynamics and Controls of Urban Heat Sink and Island Phenomena in a Desert City: Development of a Local Climate Zone Scheme Using Remotely-Sensed Inputs. *Int. J. Appl. Earth Obs. Geoinf.* **2016**, *51*, 76–90.
17. Costanzini, S.; Despini, F.; Beltrami, L.; Fabbi, S.; Muscio, A.; Teggi, S. Identification of SUHI in Urban Areas by Remote Sensing Data and Mitigation Hypothesis through Solar Reflective Materials. *Atmosp*. **2021**, *13*, 70.
18. Chen, C.; Bagan, H.; Xie, X.; La, Y.; Yamagata, Y. Combination of Sentinel-2 and PALSAR-2 for Local Climate Zone Classification: A Case Study of Nanchang, China. *Remote Sens*. **2021**, *13*, 1902.
19. Chang, Y.; Xiao, J.; Li, X.; Middel, A.; Zhang, Y.; Gu, Z.; Wu, Y.; He, S. Exploring Diurnal Thermal Variations in Urban Local Climate Zones with ECOSTRESS Land Surface Temperature Data. *Remote Sens. Environ.* **2021**, *263*, 112544.
20. Li, X.; Stringer, L.C.; Dallimer, M. The Role of Blue Green Infrastructure in the Urban Thermal Environment across Seasons and Local Climate Zones in East Africa. *Sustain. Cities Soc*. **2022**, *80*, 103798.
21. Goal 11. Sustainable cities and communities. Available online: https://www.undp.org/sustainable-development-goals/sustainable-cities-and-communities (Accessed on 15 march 2023).
22. IBGE. Cidades e Estados. Available online: https://www.ibge.gov.br/ (Access on 12 february 2023).
23. Badaro-Saliba, N.; Adjizian-Gerard, J.; Zaarour, R.; Najjar, G. LCZ Scheme for Assessing Urban Heat Island Intensity in a Complex Urban Area (Beirut, Lebanon). *Urban Clim*. **2021**, *37*, 100846.
24. Sobrino, J.A.; Irakulis, I.A. Methodology for Comparing the Surface Urban Heat Island in Selected Urban Agglomerations Around the World from Sentinel-3 SLSTR Data. *Remote Sens*. **2020**, *12*, 2052.
25. ESA. Climate Change Initiative Land Cover. Available online: https://maps.elie.ucl.ac.be/CCI/viewer/ (Accessed on 12 february 2023).
26. Liu, L.; Zhang, Y. Urban Heat Island Analysis Using the Landsat TM Data and ASTER Data: A Case Study in Hong Kong. *Remote Sens*. **2011**, *3*, 1535-1552.
27. Singh, P.; Kikon, N.; Verma, P.; Impact of land use change and urbanization on urban heat island in Lucknow city, Central India. A remote sensing bases estimate. *Sustain. Cities Soc.* **2017**, *32*, 100-114.
28. García, D.H., Díaz, J.A. Space–time analysis of the Earth's surface temperature, surface urban heat island and urban hotspot: relationships with variation of the thermal field in Andalusia (Spain). *Urban Ecosyst*, **2023**. 10.1007
29. Sharma, R.; Pradhan,L.; Kumari, M.; Bhattacharya, P.; Assessing Urban Heat Islands and Thermal Comfort in Noida City Using Geospatial Technology. *Urban Climate,* **2021**, *35* (January): 100751.
30. Naim, M.; Huda, N.; Kafy, A.; Assessment of Urban Thermal Field Variance Index and Defining the Relationship between Land Cover and Surface Temperature in Chattogram City: A Remote Sensing and Statistical Approach. *Environmental Challenges*, **2021**, *4*, 100107.
31. Magagnin, R. C., Silva, A. N.; Souza, L; Ramos, R. PLURIS 2021 - 9º Congresso Luso-Brasileiro para o Planejamento Urbano, Regional, Integrado e Sustentável - Pequenas cidades, grandes desafios, múltiplas oportunidades. Pluris 2021. São Paulo, Brazil, 07-09 April 2021.
32. Giles, B. D.; Balafoutis, C.; Maheras, P;. Too Hot for Comfort: The Heatwaves in Greece in 1987 and 1988 *International Journal of Biometeorology*, **1990**, *34*, 10.1007.
33. Thom, E.C. The Discomfort Index. Weatherwise 1959, 12, 57–61.
34. Sobrino, J.A.; Julien, Y.; García-Monteiro, S. Surface Temperature of the Planet Earth from Satellite Data. *Remote Sens*. **2020**, *12*, 218.
35. Kafy, A.; Khan, M.H.H.; Islam, A.; Sarker, H.S.; Prediction of Future Land Surface Temperature and Its Impact On Climate Change: A Remote Sensing Based Approach In Chattogram City. 1st International Student Research Conference – 2020, Dhaka, Blangladesh, 2020.
36. Dewan, A.; Kiselev, G.; Botje, D. Diurnal and Seasonal Trends and Associated Determinants of Surface Urban Heat Islands in Large Bangladesh Cities. *Appl. Geogr*. **2021**, *135*, 102533.
37. Dimitrov, S.; Popov, A.; Iliev, M. An Application of the LCZ Approach in Surface Urban Heat Island Mapping in Sofia, Bulgaria. *Atmosphere* **2021**, *12*, 1370.
38. Hu, J.; Yang, Y.; Pan, X.; Zhu, Q.; Zhan, W.; Wang, Y.; Ma, W.; Su, W. Analysis of the Spatial and Temporal Variations of Land Surface Temperature Based on Local Climate Zones: A Case Study in Nanjing, China. IEEE J. *Sel. Top. Appl. Earth Obs. Remote Sens*. **2019**, *12*, 4213–4223.
39. Cai, Z.; Tang, Y.; Zhan, Q. A Cooled City? Comparing Human Activity Changes on the Impact of Urban Thermal Environment before and after City-Wide Lockdown. *Build. Environ*. **2021**, *195*, 107729.
40. Li, X.; Stringer, L.C.; Dallimer, M. The Role of Blue Green Infrastructure in the Urban Thermal Environment across Seasons and Local Climate Zones in East Africa. *Sustain. Cities Soc*. **2022**, *80*, 103798.

 doi:10.20944/preprints202304.0045.v1

41. Purio, M.A.; Yoshitake, T.; Cho, M. Assessment of Intra-Urban Heat Island in a Densely Populated City Using Remote Sensing: A Case Study for Manila City. *Remote Sens*. **2022**, *14*, 5573.
42. MAPBIOMAS. Coleções Mapbiomas. Avaiable online: https://mapbiomas.org/colecoes-mapbiomas-1?cama_set_language=pt-BR. (Acessed on 28 February 2023).
43. SUDEMA. Jardim Botânico Benjamin Maranhão. Available online: https://sudema.pb.gov.br/servicos/servicos-ao-publico/jardim-botanico (Accessed on 15 February 2023).
44. Siami, L.; Ramadhani, A; Climatology of Discomfort Index for Decade in Bandar Lampung, Indonesia. *KnE Social Sciences*, **2019**, *3*, 460-469.
45. Md Din, M. F.; Lee, Y.Y.; Ponraj, M.; Ossen, D.R.; Iwao, K.; Chelliapan, S.;Thermal Comfort of Various Building Layouts with a Proposed Discomfort Index Range for Tropical Climate. *Journal of Thermal Biology*, **2014**, *41*, 6–15.